

Simulation of process for electrical energy production based on molten carbonate fuel cells

G. De Simon^{a,b,*}, F. Parodi^b, M. Fermeglia^a, R. Taccani^a

^aUniversity of Trieste, via Valerio 10, 34127 Trieste, Italy

^bAnsaldo Fuel Cells S.p.A., Corso Perrone 25, 16152 Genova, Italy

Received 31 May 2002; received in revised form 22 November 2002; accepted 2 December 2002

Abstract

A global molten carbonate fuel cells (MCFC) power plant steady-state simulation is presented. A performance fuel cell numerical model is developed and integrated as a custom block in Aspen plusTM for the whole process simulation. The burner/reformer compact unit is built assembling existing Aspen plusTM internal blocks. A simulation is obtained with the preliminary input specification to get to the base case and a sensitivity analysis is conducted, in order to find the process parameters whose change improves the global efficiency.

© 2003 Elsevier Science B.V. All rights reserved.

Keywords: Fuel cells; Molten carbonate fuel cell; Simulation; Power-generation system

1. Introduction

Fuel cells are high efficiency and low polluting electrochemical devices, meant to convert the hydrogen chemical energy directly into electrical energy [1–3]. The use of fuel cells in power generation plants is spurred by many factors such as [4]:

- the need of pollution reduction;
- the threat of near irreversible and fast oil prices rise;
- the wish of many countries to reduce foreign energy dependency.

On the other hand, still some problems has to be solved in order to enable the commercial diffusion of fuel cells. First of all manufacturing costs have to be reduced and, at the same time, lifetime of the equipment has to be increased.

Many types of fuel cells have been developed so far. The widest classification divides them on the basis of operating temperature. High temperature fuel cells, such as molten carbonate fuel cells (MCFC), have the following advantages:

1. No need for expensive and easily poisoning catalysts (Pt based).

2. High operating temperature (about 650 °C) which enables efficient recovery of residual pressure and waste heat via gas turbine bottoming cycle and cogeneration.

But focusing the attention in the energy production process exclusively on fuel cells is very restrictive since they can not produce power on their own due to the fact that hydrogen in nature is not present in enough quantity. Therefore, the fuel must be obtained from primary sources, which at present time are mainly fossil fuels (e.g. oil or natural gas). For this reason a reforming unit is needed to convert primary fuels in hydrogen, that can later be fed to the fuel cells. Fuel cells and reformers are not the only units needed in the process, some of them will be explained later in this article.

Once the behaviour of all individual devices of the process is defined, it is necessary to study their interaction, aiming at understanding which are the most important factors affecting the global efficiency.

Different studies and hypothesis have been proposed to integrate high temperature fuel cells and gas turbine (e.g. [5–7]).

In [5], the predicted performance for a 220 kW, pressurised SOFC directly coupled with a micro gas turbine is reported. The hybrid cycle shows 57% expected efficiency.

Ref. [6] reports performance predicted for a 20 MW, ambient pressure, internal reforming MCFC-based power

* Corresponding author.

E-mail addresses: desimon@ari.ansaldo.it, desimon@adriacom.it (G. De Simon), parodi@ari.ansaldo.it (F. Parodi), mauf@dicamp.univ.trieste.it (M. Fermeglia), taccani@univ.trieste.it (R. Taccani).

Nomenclature

E	cell Nernst voltage (V)
P_{chemical}	chemical power of the inlet fuel (kW)
$P_{\text{compressor}}$	compressor consumption (kW)
P_{stack}	stack electrical power (kW)
P_{turbine}	turbine power (kW)
R_c, R_e, R_p	resistance parameters ($\Omega \text{ cm}^2$)
R_{int}	total internal resistance ($\Omega \text{ cm}^2$)
V	cell voltage (V)

plant fuelled with natural gas. In that case, the gas turbine is coupled with the fuel cells via heat exchangers and the expected efficiency of the system is about 75%. Similar results are stated for 1 MW size on [7].

Ref. [8] shows a plant configuration similar to the one discussed in this work, 250 kW range, ambient pressure, internal reforming MCFC-based power plant fuelled with natural gas. That system operates at ambient pressure without coupled gas turbine. In that case real measured efficiencies are in the range of 47% net.

On the other hand, the processes reported in the literature are very different both for the fuel cell technology used and for the system configuration adopted. Therefore, a direct comparison can not be made and also a comparison-based only on the expected electrical efficiency can be confusing. Furthermore, some extrapolation and simplification of the models have been made in particular when MW range are considered.

The aim of this work is to maintain a low profile on expectations but base the work on real data coming from experimental experience of the authors and using detailed model for the fuel cell section to account for the real operating conditions of the cells.

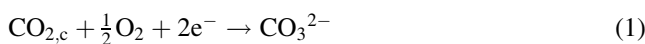
The process studied is a 500 kW MCFC power system, based on Ansaldo fuel cells (AFC) technology [9–11].

A numerical steady-state simulation of the process is set up and a detailed model of the fuel stack is developed and interfaced with the commercial software Aspen plusTM for the global system simulation.

2. Single fuel cell model

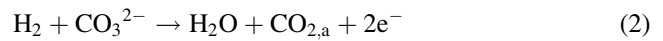
2.1. Molten carbonate fuel cell

Fig. 1 shows the essential geometry of a single cell and the main components, that are: (1) *two metal current collectors*, whose task is also to distribute the gas streams across the electrodes surfaces; (2) *a NiO-based porous cathode*, where the following reduction reaction occurs:

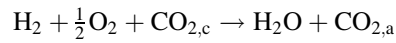


producing the CO_3^{2-} ion, that must travel across an (3) *electrolyte tile* (made up by molten K, Na and Li carbonates in a solid porous and inert matrix) and reach a (4)

Ni-based porous anode, where oxidation occurs:



The total reaction, sum of (1) and (2), is



which is essentially the hydrogen combustion reaction combined with a CO_2 transfer from cathode (c) to anode (a).

The model development for the simulation of fuel cell is accomplished in two steps:

1. Describe the cell behaviour in any point of the surface, where temperature, pressure and gas composition are fixed.
2. From results of first step, build a global performance model considering that local conditions change along the surface.

The use of this kind of model for plant simulation purposes, has the following main advantages:

- It is possible to access the temperature of the solid,
- The heat produced inside the cell can be split between the anodic and cathodic gases by means of heat transfer calculations.

2.2. Local model

Model simplifications based on some assumptions are introduced in the simulation in order to reduce the CPU time without losing in accuracy and reliability.

Models of cell local kinetics, such as the one reported in [12,13], has not been considered in this work, due to the complexity of the set of differential equations. The semi-empirical model reported in [14] was considered. The local behaviour is described as a simple electrical circuit, series of an ideal voltage, determined by the *Nernst equation*, and an internal resistance, made up by the sum of the three contributions: contact resistance (R_c) between electrode and current collector, electrolyte tile Ohmic resistance (R_e) and polarisation contribution (R_p). The first term was found to be simply a constant ($R_c = C$), the second term is an exponential function of temperature and the last one depends on both temperature and partial pressures of the species involved in the electrochemical reaction. All coefficients of this model come from [14], obtained by experimental data fittings. In conclusion, real voltage can be simply determined from Ohm's law:

$$V = E - R_{\text{int}}J \quad (3)$$

where J is the current density (mA/cm^2), R_{int} the internal resistance, equal to $R_c + R_e + R_p$ ($\Omega \text{ cm}^2$), and E is the Nernst ideal voltage (V).

2.3. Performance model: the extended cell

The main assumptions considered in the model development are

- (i) steady state conditions;

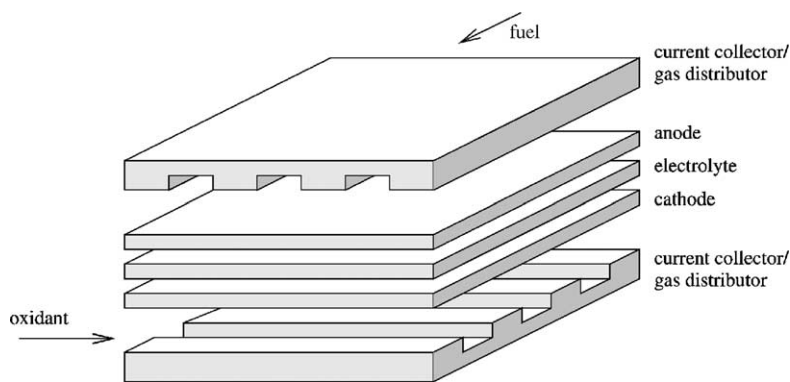


Fig. 1. Sketch of a fuel cell.

- (ii) the anodic electrochemical reaction was neglected $\text{CO} + \text{CO}_3^{2-} \rightleftharpoons 2\text{CO}_2 + 2\text{e}^-$ for its very low rate;
- (iii) non-limiting diffusion in macro-pores of the electrode and in gas stream;
- (iv) current collector as an ideal conductor (constant voltage on whole surface);
- (v) adiabatic conditions;
- (vi) water gas-shift reaction ($\text{CO} + \text{H}_2\text{O} \rightleftharpoons \text{CO}_2 + \text{H}_2$) considered at the equilibrium for its high rate;
- (vii) ideal gas.

It is important to note that diffusion phenomena occur at high reactants utilisation and reduce heavily the device efficiency; for this reason they must be avoided, by defining the cell working conditions in terms of gas utilisation such as diffusion is negligible. So assumption (iii) is justified.

The model considers local temperature, pressure and composition changes along gases path in the ducts, because of reactions, heat transfer and pressure drop. To find global cell behaviour it is necessary to solve simultaneously four sets of equations (a similar work was already done in [14,15]):

1. Mass balance (for each gas component).
2. Momentum balance (of cathode and anode gas streams).
3. Energy balance.
4. Local kinetics.

The boundary conditions are input gas streams temperature, pressure and composition, and the assumption of adiabatic conditions. For the numerical solution, finite difference and relaxation methods have been employed and implemented in Fortran 90 language.

3. Process simulation

The process simulation was performed by Aspen plusTM. Default Aspen plusTM models have been used for traditional plant units, while for fuel cells stack a custom Fortran 90 code was developed in this work.

3.1. Process flow sheet

Fig. 2 reports a general flow sheet of the simulate process, while Fig. 3 reports details of the electrochemical module.

Natural gas, after a primary treatment, is mixed with steam, pre-heated in a regenerative heat exchanger and fed to the reformer, where CO and H₂ are produced. Exit gas passes again through regenerative exchanger, set ready to be processed at the anodic side of the fuel cells stack. After electrochemical and gas shift conversion, residual concentration of fuel is still present, because CH₄ not converted in the reformer pass inert the stack and because, to avoid diffusion control in the electrochemical process, not all H₂ and CO is consumed. So fuel containing effluent is mixed with part of cathodic exhaust (comburent) and fed to a catalytic burner where the heat necessary for endothermic reactions taking place in reforming process is produced and directly exchanged. CO₂ rich and hot gas is mixed with fresh air coming from compressor and fed to the cathode where O₂ and CO₂ are consumed by reaction (1).

Part of cathode exhaust gas is sent to a turbine for recovering residual energy, which is used to drive air compressor and to produce further electrical energy. The hot effluent finally release the heat necessary to produce reforming steam and for a possible cogeneration.

3.2. Models of the plant components

3.2.1. Reformer and catalytic burner

These two units are assembled together in the “Modular Integrated Reformer” (MIR): it consists of a compact heat exchanger with one side filled with reformer catalyst and the other with burning catalyst.

No predefined unit was available in Aspen plusTM libraries, so a well approximating scheme has been assembled using standard units. The model divides the unit geometrically in four parts, alternating the two reactions and heat exchanges, thus, simulating the simultaneity of the three processes taking place in the MIR. The four reformer

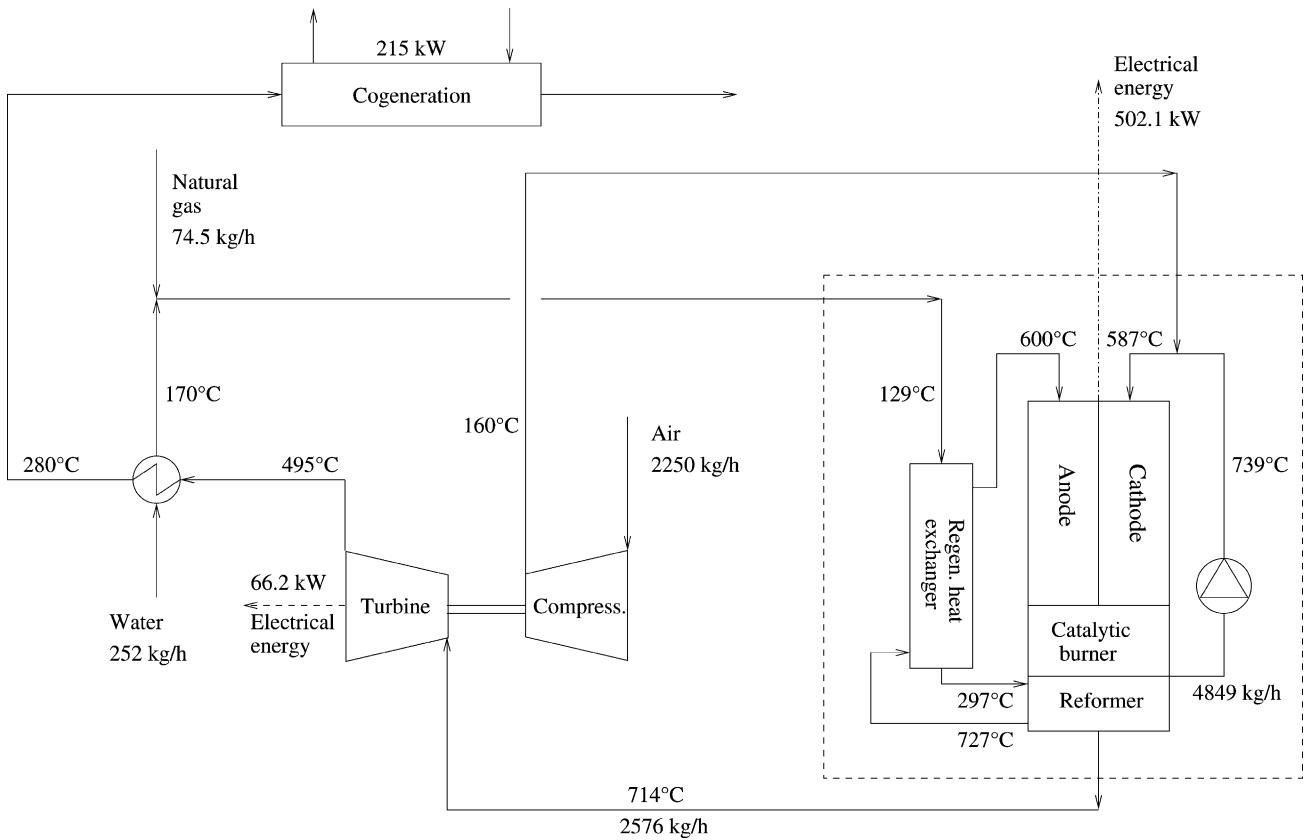


Fig. 2. Process flow sheet with numerical results of the “precombustion case” (see Section 4.2.3).

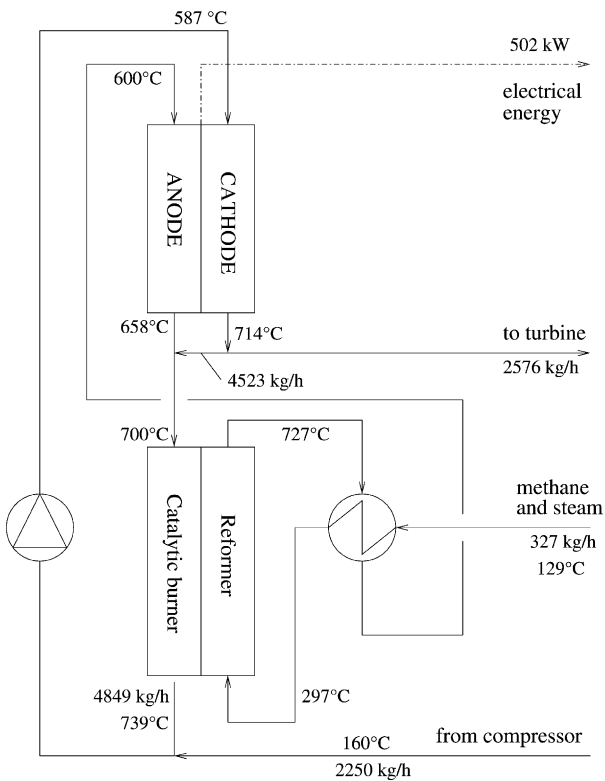
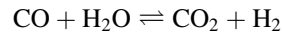
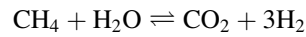


Fig. 3. Electrochemical module with numerical results of the “precombustion case” (see Section 4.2.3).

reactors (left side of Fig. 4) are in chemical equilibrium for methane reforming and gas-shift reactions:



Reactors on the right side partially burn H_2 , CH_4 and CO until total consumption of the fuel is reached in the last unit.

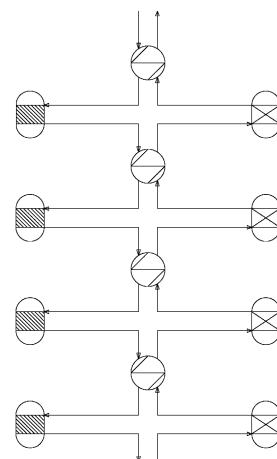


Fig. 4. MIR approximative model.

3.2.2. Fuel cells stack

Likewise, the MIR, also a fuel cells stack model was not available in the library of units. In this case, the user model developed in this work (see Section 2.3) was employed, interfacing the Fortran 90 code with the process simulator.

The parameters required by the simulation code as well as the equations for the semi-empirical internal resistance (3) are derived from [14] and are based on AFC experimental tests.

Stacked cells are considered having the same behaviour as stand alone, so heat exchange between adjacent cells is neglected. Without this simplification the number of unknown variables to be solved for would be multiplied by the number of cells assembled in the stack, increasing exponentially the numerical complexity and computing time. This assumption does not introduce relevant approximation, as confirmed in [9].

3.2.3. Compressor, turbine and blower

These units have been simulated by predefined blocks with fixed isentropic and mechanical efficiencies, employing typical values of existing units of similar size.

3.2.4. Heat exchangers

For regenerative heat exchanger the hot gas exit temperature has been fixed at 600 °C, the other exit temperature is calculated from energy balance; the same choice for the steam generator, where vapour temperature have been fixed to 170 °C, free to be changed in plant analysis.

3.2.5. Cogeneration apparatus

For the aims of this work cogeneration does not represent a constraint: all residual heat of the effluent is exploited until exit temperature reaches about some tens of degrees over ambient conditions.

3.3. Main assumptions

Pressure drop of the various devices (except for the one of fuel cells) and heat losses towards surroundings have been neglected. The main pressure drops are located at the stack and at the MIR: in the latter it has been estimated an order of magnitude of 1 kPa per side (reformer and catalytic burner).

Approximation about heat losses is justified by the fact that all devices are contained in an high temperature vessel insulated with very low conducting materials.

4. Results and discussion

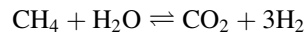
4.1. Preliminary considerations

Before considering the results obtained for the global process, it is useful to point out some introducing aspects.

Fuel cells efficiency is defined as the ratio of electric power produced by the stack and chemical power of the fuel

actually consumed. Referring the efficiency to total input fuel energy could be misleading because residual fuel is doubly recovered. In the catalytic burner part of the heat produced is transferred to the reformer, where it is converted to chemical energy by means of endothermic reactions; another part of gas energy is next recovered in the turbine. These two energy recovers take place with less efficiency than fuel cell conversion (see later), hence, to achieve high global efficiency, it is useful to assign most possible energy to electrochemical conversion.

The *reforming* reaction:



is endothermic and with an increase of number of moles, so an increase of temperature and a pressure reduction foster the equilibrium towards products, improving the reforming process.

The process can be considered a fuel cell/gas turbine hybrid cycle (FC/GT), where topping cycle is FC and bottoming one is GT. It is useful considering the variables that affect bottoming cycle behaviour. For a gas turbine system the efficiency is improved by high pressure ratio (output/input compressor pressures) and high turbine input gas temperature. In the present case, FC and MIR substitute the combustion chamber, but the qualitative trend remains unchanged.

4.2. Base case

The simulation starts with the process “base case” in which all the assumptions used as preliminary project specifications are used. Then changes will be made to base case aiming at finding which of them improve the global efficiency.

4.2.1. Input specifications

In order to have a reference for comparing the results of the different simulation runs, the set of boundary conditions reported in Table 1 has been selected.

They represent proper operating conditions for the present technology of MCFC stacks and are included on the operating conditions forecasted by AFC for the “Series 500” Demo Plant [16]. Most of them has been successfully demonstrated on full area short stacks [17].

A fixed temperature of the solid parts of the cells (650 °C) is obtained varying the input cathode gas temperature. Cathodic gas temperature is controlled by adjusting the oxidant exhaust recirculation ratio, exploiting hot gas sensible heat, which raises the temperature of the fresh air, after mixing.

Another constraint is the steam to methane ratio: it must be more than 3 to avoid carbon deposition, that inhibits catalyst activity (see [1]).

As already underlined, for a better global efficiency, it is useful to convert the energy inside the fuel cells stack, rather than in the turbine. Therefore, high fuel utilisation is desired

Table 1
Input specifications

Cell solid temperature (°C)	650
Fuel utilisation (%)	75
Oxygen utilisation (%)	30
Pressure (bar)	3.5
Steam/methane ratio	3
Steam temperature (°C)	170

through the electrochemical device. On the other hand, diffusion phenomena have to be avoided, so H₂ + CO utilisation in the stack up to 75% is selected. This value is obtained varying the plant methane feed rate.

The fresh air flow rate has to be adjusted to be enough for electrochemical consumption and for the combustion of anode exhaust gas. For the base case a flow rate for 30% of oxygen utilisation in the stack is selected.

4.2.2. Base case results

Table 2 reports a summary of the main results of base case. Stack efficiency is defined as the ratio of electrical energy produced and the chemical energy of the fuel consumed inside the electrochemical device.

The bottoming cycle efficiency is computed as:

$$\frac{P_{\text{turbine}} - P_{\text{compressor}}}{P_{\text{chemical}} - P_{\text{stack}}}$$

where P_{turbine} is the power produced by the turbine, $P_{\text{compressor}}$ the compressor consumption, P_{chemical} the energy introduced with input methane based on lower heating value, and P_{stack} the electricity produced by the fuel cells stack. The denominator represents the residual energy after electrochemical conversion. The bottoming cycle efficiency obtained is about, 12%, far from usual values that can be obtained with gas turbine systems: in fact operating pressure (3.5 bar) and inlet turbine gas temperature (less than 700 °C) are optimised for fuel cells stack and not for bottoming cycle.

Cogeneration efficiency is defined as total power produced (electrical + thermal) divided by P_{chemical} .

An analysis of Table 2 shows that the total efficiency differs a lot from the fuel cells one (51.1% versus 60.3%).

Table 2
Base case results

CH ₄ plant feed rate (kg/h)	82
Stack power (kW)	505.6
Bottoming cycle power (kW)	77.5
Thermal cogeneration power (kW)	261
Reforming temperature (°C)	688
CH ₄ conversion (%)	79.3
Stack efficiency (%)	60.3
Cell voltage (V)	0.769
Bottoming cycle efficiency (%)	12.2
Global process electrical efficiency (%)	51.1
Cogenerative efficiency (%)	74

The reason has to be found in the low CH₄ conversion in the reformer (79.3%), causing a lot of energy contained in the methane to pass non-converted through fuel cells, only partially recovered by heat exchange with reformer and by gas turbine (see Section 4.1). Usually, to obtain higher conversion in industrial reforming processes, the final temperature is raised at more than 800 °C, to improve chemical equilibrium while in the present case it is only 688 °C. This is mainly due to the fact that the combustion takes place gradually from the inlet to the outlet, so the burned gas, and consequently the reformer gas, can not reach suitable temperature.

4.2.3. Precombustion

A way to increase the conversion is to burn all the residual fuel coming from the stack before the heat exchange with the gas to be reformed, hence, inlet temperature of the heating medium will be higher. In the simulation this is achieved setting unitary conversion in the first burner encountered by the gas in Fig. 4. In this way, a faster heat transfer which raise outlet reforming temperature up to 727 °C is obtained. The new results (see Table 3 and Figs. 2 and 3) show indeed a better CH₄ conversion and consequent nearer stack and global efficiencies, the latter increased by less methane consumption. A comparison between Tables 2 and 3, shows that in spite of a constant stack and bottoming cycle efficiency, the global one improves: in fact after the modification, the stack power remain almost constant, bottoming and thermal power decrease. Consequently more power conversion takes place in the fuel cells where efficiency is high. On the other hand, the cogeneration efficiency decreases, because the residual energy is more degenerated (inlet temperature in the cogeneration heat exchanger 280 °C versus 300 °C without precombustion).

The new configuration is assumed to replace the base case for the advantages gained with precombustion.

4.3. Sensitivity analysis

The sensitivity analysis considers the base case and varies some important parameters of the process.

Table 3
Results of the pre-combustion case

CH ₄ plant feed rate (kg/h)	74.5
Stack power (kW)	502.1
Bottoming cycle power (kW)	66.2
Thermal cogeneration power (kW)	215
Reforming temperature (°C)	727
CH ₄ conversion (%)	88.7
Stack efficiency (%)	59.7
Cell voltage (V)	0.761
Bottoming cycle efficiency (%)	12.4
Global process electrical efficiency (%)	54.8
Cogenerative efficiency (%)	75.6

Table 4
H₂O/CH₄ sensitivity analysis

H ₂ O/CH ₄	3	4	4.5	5.5
Electrical plant efficiency	54.8	56.3	57.1	57.7
Stack efficiency	59.7	58.8	58.3	57.5
Cell voltage	0.761	0.748	0.741	0.730
CH ₄ conversion	88.7	92.3	94	96.6
Bottoming cycle efficiency	13.2	14.3	14.8	16.2
Cogenerative efficiency	75.6	71.8	69.8	65.8

4.3.1. Steam to methane ratio

Table 4 shows the effect of an increase in the steam to methane ratio on the main parameters of the process. An increase in the input water results in an improvement of the reforming and gas shift equilibrium, because the amount of one of the reactants is increased, as can be seen in the methane conversion data. In spite of a slight fuel cells efficiency reduction, due to reactants dilution, the global electrical efficiency improves. The main factors explaining

this behaviour are (i) more energy is converted in the stack for a higher amount of hydrogen available, (ii) more heat is removed from effluent gas, so more heat is recycled into the plant and in the bottoming cycle, increasing its efficiency (see bottom part of Table 4). As usual for an heat engine, an higher GT cycle efficiency means that the residual heat is entropically degenerated. Therefore, its temperature is lower and cogenerative efficiency is reduced.

4.3.2. Pressure

The effect of pressure on fuel cells can be seen in Fig. 5 where the results of an example of a single fuel cell simulation (explained in Section 2) is illustrated: by increasing operating pressure, the voltage/current density curve moves upwards; as can be noted the improvement is weaker when pressure becomes higher. It is well-known that high operating pressures affects positively also the bottoming cycle, while the reforming is worsened, because chemical equilibrium is shifted to the reactants. Fig. 6 reports the results of sensitivity analysis on pressure, and it shows that

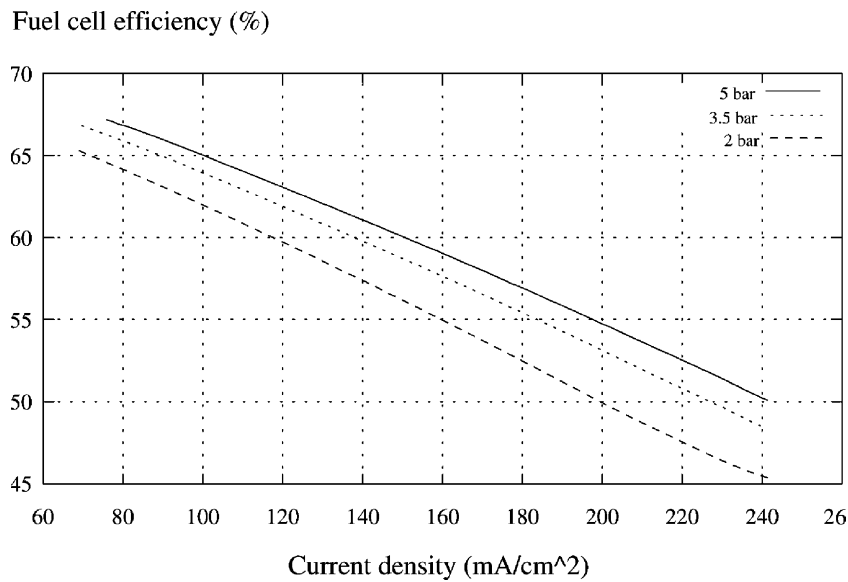


Fig. 5. Pressure effect on fuel cell.

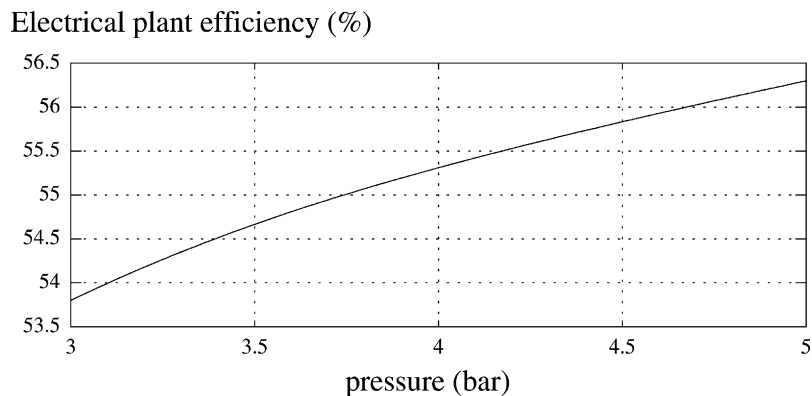


Fig. 6. Pressure sensitivity analysis.

Electrical plant efficiency (%)

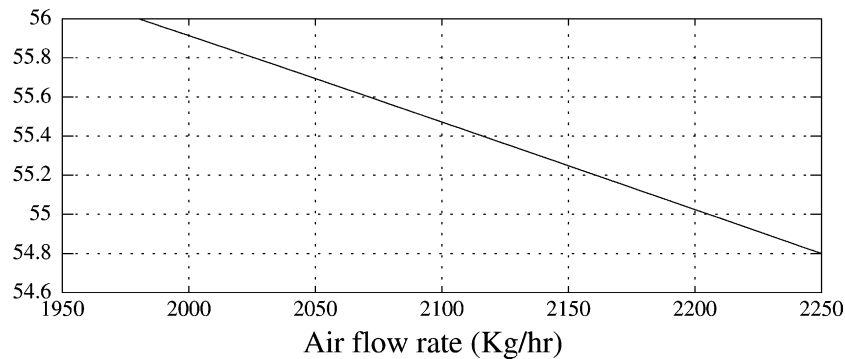


Fig. 7. Air flow rate sensitivity analysis.

Table 5
Air flow rate sensitivity analysis results

Air flow rate (kg/h)	Recirculation (%)	Reforming temperature (°C)	CH ₄ conversion (%)
1980	55.7	742	91.4
2050	57	740	91.1
2250	60	727	88.7

the increase of the two cycles efficiencies overcomes methane conversion effect. There is a worsening of cogeneration, because residual heat exits again in a more degenerated form.

4.3.3. Air flow rate

The fresh air flow rate does not show any changes of cells, bottoming cycle and cogenerative efficiencies. The graph in Fig. 7 shows a reduction in global electrical efficiency as air flow rate is increased. The explanation of this phenomenon has to be found in the chain of effects happening inside the process (see Table 5): more input fresh air means more refrigeration on the stack; to keep the cells temperature constant at 650 °C, an higher exhaust recirculation ratio is needed; and higher amount of air is sent at the catalytic burner. Consequently more sensible heat is brought in the MIR for the reformer, but, most important, the burned gas is diluted reducing its temperature and consequently the reforming one.

5. Conclusions

The main steps of this work are

- the development of a fuel cell numerical model, implemented in Fortran 90, on the base of [14];
- the development of a reformer/burner unit model employing existing blocks in Aspen plusTM;
- the assembling of a model for the complete system using the custom and Aspen plusTM library blocks;

- the study of the base case, driven on preliminary input specifications;
- the sensitivity analysis on the main variables defining the process.

The simulation of the fuel cell has enabled the deep understanding of the electrochemical device behaviour, useful for its integration with the other units. The simulation of the plant has evidenced the main interactions among the various devices. Calculations show that global electrical efficiency surely can be kept easily over 50–55%, derived from about 60% of fuel cells stack and 12% of the bottoming cycle. Cogenerative efficiency in the simulation remains instead within 75%.

It was found that if the anode exhaust gas is burned before heat exchange with the reformer, a higher conversion is obtained and the global electric and cogenerative efficiencies rises, respectively, from 51.1 and 74 to 54.8 and 75.6%.

These results agree with expectations for similar systems [5] and seems to predict better performance respect to experimental results for ambient pressure system without GT integration [8].

The sensitivity analysis showed that there is still room for improvement in electrical efficiency by increasing steam to methane ratio, pressure and decreasing air feed rate. All these variables, at the same time, cause often the cogeneration worsening.

The simulation results encouraged AFC to carry on with the planned “MCTWINS project” partially funded by the European Community [18]. The project goal is to design, build and test a DEMO Plant named “Series 500” based on MCFC technology and using a similar plant configuration to that discussed above.

References

- [1] K. Kordesch, G. Simader, Fuel Cells and Their Application, VCH, 1992.
- [2] A.J. Appleby, F.R. Foulkes, Fuel Cell Handbook, Van Nostrand Reinhold, New York, 1989.

- [3] J.H. Hirschenhofer, D.B. Stauffer, R.R. Engleman, M.G. Klett, Fuel Cells Handbook, FETC, November 1998.
- [4] R. Singh, Will Developing Countries Spur Fuel Cells Surge? Chemical Engineering Progress, March 1999.
- [5] R.A. George, Status of tubular SOFC field unit demonstrations, J. Power Sources 86 (2000) 134.
- [6] H. Maru, et al., Direct Fuel Cell/Turbine Hybrid System for Ultra High Efficiency Power Generation, Abstracts of the VII Grove Fuel Cell Symposium, London, September 2001.
- [7] E. Liese, R.S. Gemmen, Dynamic modelling results of a 1 MW MCFC/GT power system, in: Proceedings of the ASME Turbo Expo 2002, Amsterdam, 3–6 June 2002.
- [8] M. Gnann, The MTU Fuel Cell Hot Module Cogeneration Unit 250Kee, Abstracts of the VII Grove Fuel Cell Symposium, London, September 2001.
- [9] B. Bosio, P. Costamagna, F. Parodi, B. Passalacqua, Industrial Experience on the development of the molten carbonate fuel cell technology, J. Power Sources 74 (1998) 175–187.
- [10] Molten Carbonate Fuel Cell 100 kW Cogeneration Powew Plant, ENERGIE, 1999.
- [11] MCFC “Series 500” Twinstack Powered First-of-a-Kind, ENERGIE.
- [12] J.O’M. Bockris, S. Srinivasan, Fuel Cells: Their Electrochemistry, McGraw-Hill, New York, 1969.
- [13] G. Wilemski, Simple porous electrode model for molten carbonate fuel cells, J. Electrochem. Soc. 130 (1983) 117–121.
- [14] B. Bosio, P. Costamagna, F. Parodi, Modelling and experimentation of molten carbonate fuel cell reactors in a scale-up process, Chem. Eng. Sci., vol. 54, 1999, pp. 2907–2916.
- [15] T.L. Wolf, G. Wilemski, Molte carbonate fuel cell performance model, J. Electrochem. Soc. 130 (1983) 48–55.
- [16] MCFC Series 500 TwinstackTMPowered First-of-a-Kind, European Commission Report No. EUR19368; p. 23; ISBN 92-828-9419-3, Luxembourg, 2000.
- [17] Development of Industrially Relevant MCFC Stacks (DIREM), European Commission Report No. EUR19368; p. 15; ISBN 92-828-9419-3, Luxembourg, 2000.
- [18] European Fuel Cell Projects 1995–2000, European Commission Report No. EUR19368; p. 23; ISBN 92-828-9419-3, Luxembourg, 2000.